

# MULTI-PATCH AGGREGATION MODELS FOR RESAMPLING DETECTION

Mohit Lamba      Kaushik Mitra

Department of Electrical Engineering, Indian Institute of Technology Madras

## ABSTRACT

Images captured nowadays are of varying dimensions with smartphones and DSLR's allowing users to choose from a list of available image resolutions. It is therefore imperative for forensic algorithms such as resampling detection to scale well for images of varying dimensions. However, in our experiments we observed that many state-of-the-art forensic algorithms are sensitive to image size and their performance quickly degenerates when operated on images of diverse dimensions despite re-training them using multiple image sizes. To handle this issue, we propose two novel deep neural networks — *Iterative Pooling Network (IPN)*, which does not assume any prior information about the original image size, and *Branched Network (BN)*, which uses this prior knowledge to produce better results. *IPN* adopts a novel *iterative pooling* strategy that converts tensors of multiple sizes to tensors of a fixed size, as required by deep learning models with fully connected layers. *BN* alternatively adopts a branched architecture with dedicated pathways for images of different sizes. The effectiveness of the proposed solution is demonstrated on two problems, resampling detection and photorealism detection, which are generally solved as independent problems with different deep learning models. The code is available at <https://github.com/MohitLamba94/Iterative-Pooling>.

**Index Terms**— Post JPEG resampling detection, photorealism detection, pooling, variable image dimensions

## 1. INTRODUCTION

Resampling detection has been one of the extensively studied topics because any type of image manipulation often involves this operation [1, 2, 3, 4]. The earlier works focused on uncompressed images [1] or considered just upsampling [5] but a more realistic scenario would involve double compressed images [2, 3], once at the time of acquisition and then again while saving the image after manipulation. The case of compressed images with resampling is complicated because it results in non-aligned compression [6] where compression traits camouflage with resampling traits. More critical however is the fact that many compression techniques such as JPEG2000 can tile the image in blocks of arbitrary sizes. In many standard implementations, such as MATLAB JPEG2000 encoder,

this block size is as big as the entire image. Thus, for detecting resampling the input patch size should be chosen based on the image size. However, this is not possible for neural networks with fully connected (*fc*) layers [4, 7], the most popular choice for classification nowadays.

Another problem with operating on patches of fixed size, say  $128 \times 128$ , is that it may be the optimum choice for images of dimension, say  $512 \times 512$ , but it is too small for images of larger dimensions, say  $4000 \times 4000$ . This is illustrated in Fig. 1. On the other hand one can always choose a large patch size for better performance. But the downside of this choice is that it won't work for smaller image sizes and the algorithm would incur excessive computations and processing time and poor manipulation localization [8, 9]. It is perhaps for this reason that many recent works have considered images of roughly the same size and consequently a fixed patch size. Refer to Table 1 for some of the recent works with their choice of image and patch sizes. Our experiments show that the performance of these algorithms quickly degenerate when operated on images of varying dimensions.

To handle the issue of variable image size, we propose two deep neural networks — *Iterative Pooling Network (IPN)*, that assumes no prior information about the original image size and *Branched Network (BN)* that assumes some information about the same. *IPN* integrates the proposed *iterative pooling* strategy to existing deep neural networks which transforms variable patch sizes to fixed-size tensors before passing them to the *fc* layer of the network. *BN*, on the other hand, requires coarse level information about image sizes to separately process images of different size for better performance. We show that by leveraging on pre-trained models, the fine-tuning of the proposed networks not only converges much faster than recent works such as [4, 7] but also generalizes well for other tasks like photorealism detection of heterogeneous origin [10].

## 2. ITERATIVE POOLING

Patches of different sizes result in feature maps (tensors) of different sizes at various layers of a neural network. This is alright for convolution layers which can operate on tensors of any height and width but it is problematic for the fully connected layers. One possible solution, as adopted by Faster RCNN [11], is to max pool [12, 13] the incoming tensor with

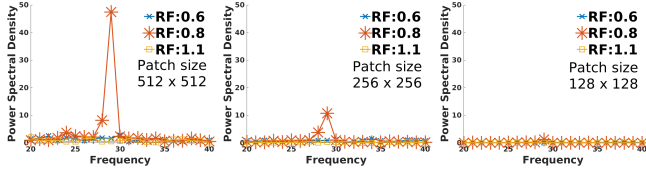


**Fig. 1.** Resampling factor (RF) estimation, using a recently proposed method by Sahu and Okade [3], for a double JPEG compressed image of size  $1024 \times 1024$  and resampled by 0.8. The performance is evaluated on 3 patch sizes. Since the accuracy is contingent on the sharpness of peak, it is observed the performance of the method quickly degrades for patches less than  $512 \times 512$ .

**Table 1.** Recent works with image size in their dataset and the corresponding patch size.

Work	Image Size	Patch Size
Sahu <i>et al.</i> [3]	$1024 \times 1024$	$512 \times 512$
MISLnet [7]	$256 \times 256$	$256 \times 256$
Li <i>et al.</i> [14]	$512 \times 512$	$512 \times 512$
Verma <i>et al.</i> [9]	$512 \times 384$	$128 \times 128$
Kirchner <i>et al.</i> [15]	$1024 \times 1024$	$512 \times 512$
Bianchi <i>et al.</i> [2]	$1024 \times 1024$	$512 \times 512$
Quan <i>et al.</i> [10]	$<1024 \times 1024$	$233 \times 233$

kernel size proportional to tensor’s height and width to reduce all tensors to the same size. However, in our experiments this resulted in poor performance, see results for the Max-Pooling Network (MPN) in Table 3. This is most likely due to the heavy loss of information which happens due to max-pooling. As an illustration, assume that the the incoming tensor is of size  $H \times H \times C$  and the expected output dimension is  $h \times h \times C$ . Then the number of data points discarded in max-pooling is given by  $(H^2 - h^2)C$  with one data point retained in every  $\frac{H^2}{h^2} \times \frac{H^2}{h^2} \times 1$  sub-block. Hence, if  $H = 16$ ,  $C = 128$  and  $h = 4$ , the number of data points discarded is around  $40k$ . To avoid this heavy information loss, we propose a new pooling strategy called *iterative pooling* which significantly boosts the classification accuracy by discretizing the space of patch dimensions but with minimal loss in information. *Iterative pooling* downsizes the input tensor by iteratively convolving it with a  $3 \times 3 \times C$  kernel with a stride of 2 for  $\log_2(\lceil \frac{H}{h} \rceil)$  iterations. The convolution weights are shared across the patch sizes and across the time steps. In each time step the height and width of the tensor reduces by half. Since the operation is carried out for logarithm time steps, with  $\frac{H}{h}$  being a small number, the operation completes almost instantaneously.

Inspired by the immense success of works like Faster RCNN [11] and YOLO [16] which decided to build on top of existing CNN models, we also chose to use ResNet-18 [17] as our base architecture. Although proposed much earlier than recent CNN models for image forensic [4, 7, 10] we

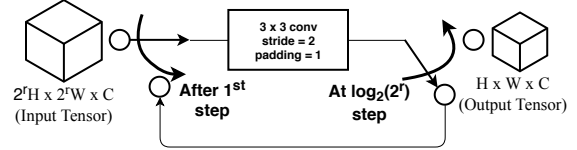


**Fig. 2.** A pictorial representation of the proposed *iterative pooling* strategy that is integrated into the proposed deep neural network, Iterative Pooling Network (IPN), to handle patches of multiple sizes which was not possible traditionally. Despite its simplicity it helps achieves much higher accuracy as confirmed in our experiments.

found that ResNet-18 with our iterative pooling strategy produces much better results. Also, the pre-trained ResNet-18 model significantly improves the convergence time of our algorithm. We inserted the proposed *iterative pooling* strategy in between the  $conv3_x$  and  $conv4_x$  layers of ResNet-18 to handle patches of varying dimension. In our experiments,  $h$  was fixed at 4.

*Iterative pooling* can result in tensors with a non-integer dimension requiring appropriate padding before convolution. This problem is also common to naive max-pooling strategy discussed above. To avoid this, we discretize the input patch space and accept patch sizes which can be expressed as some integer power of two, i.e.,  $2^r$ , see Fig. 2. This discretization is not a serious limitation for the classification task. The given patch sizes suffice for images of various dimensions and are suitable approximations of the desired value of patch dimension. For example, it is very unlikely that the performance with a patch size of  $300 \times 300$  should outperform the performance of a deep neural network with a patch size of  $256 \times 256$ . We call this architecture *Iterative Pooling Network (IPN)*.

Motivated by the idea of using a recursive block in between an otherwise feedforward neural network, we propose another solution in the next section called *Branched Network (BN)* which further helps to boost the accuracy provided some prior information about the original image size is given to the network.

### 3. BRANCHED NETWORK

In some forensic applications such as dealing with CCTV footage we have a coarse idea of the image size. This idea was however not harnessed in the previous section and we shall show in our experiments that utilizing this information further helps to boost the performance. We divide the images into three categories, namely, category I, II and III for small, medium and large-sized images respectively. These image sizes refer to image dimensions before resampling. Fixed patch size is used for each category irrespective of the resampling factor. Category I uses a patch size of  $64 \times 64$ , Category II of  $128 \times 128$  and Category III of  $256 \times 256$ .

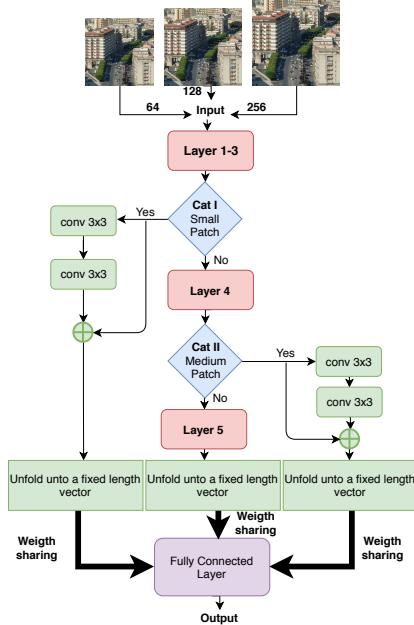


**Fig. 3.** A schematic representation of the proposed *Branched Network (BN)* for handling patches of different sizes with prior information.

Deeper thought on *iterative pooling* suggests that patches of larger size get to see the pooling kernel more number of times. If this recursive relation is unfolded it would result in a branched architecture concerning patches of multiple sizes. There is however a small issue with the way IPN does this branching which complicates the classification problem. Let’s say an image of size  $512 \times 512$  is upsampled by 1.2 and an image of size  $1024 \times 1024$  is downsampled by 0.6 factor. The resulting image size is the same for both cases and so IPN processes them identically putting the burden on fully connected layers for correct classification. The discriminatory power of the network is however enhanced if the two images were processed separately and this is the core idea for *Branched Network (BN)*. BN is given some prior information on image size before resampling and this is used to do the branching as depicted in Fig. 3. In our experiments this gives better performance than IPN.

Another naive solution is to have a separate CNN for each category. However, inspired by the success of sharing weights of the region proposal network and classification network of [11], we do not opt for this highly inefficient brute force solution. The idea is that there will be a lot of redundancy in such a system. Ordinarily, the initial layers of a CNN do some basic filtering such as edge extraction which is largely task-independent. Task-specific work is chiefly done by the later layers. Building on this intuition we successively share most of the layers and keep only one or two size-specific layers. Since size-specific layers are few, they get fine-tuned

in few iterations. The other layers are also benefitted as they are backpropagated for any resolution and so updated more frequently helping in faster convergence.

The five layers in Fig. 3 are the five convolutional layers of ResNet-18 [17]. The proposed network, called *Branched Network (BN)* is designed in such a way that the initial layers, which are task-independent, are shared by all patches. As we go deeper, the smaller patches gain sufficient receptive field and branches out. The larger patches continue together deeper till they also achieve an appreciable receptive field. Ultimately, this is followed by a common fully connected layer. The last block just before the fully connected layer consist of independent max-pooling operation to reduce the spatial resolution to  $1 \times 1$  and one-cross-one convolution to have same number of channels. They are then vectorized and fed to the fully connected layer for classification.

## 4. EXPERIMENTS

### 4.1. Dataset Preparation

We use the raw image dataset, RAISE [18], for experiments on resampling detection. We choose five image sizes:  $512 \times 512$ ,  $1024 \times 1024$ ,  $3008 \times 2000$ ,  $4288 \times 2848$  and  $4928 \times 3264$ . We use the PyTorch framework [19] for our implementation and we will make the source code public for future development.

We now describe the procedure for data preparation for image dimension  $1024 \times 1024$ . The same procedure was repeated for all other image sizes with exact split and random seed values. An uncompressed image was taken from the RAISE dataset and the central  $1024 \times 1024$  region was cropped. The image was then JPEG compressed in MATLAB by randomly choosing a quality factor from 50 to 100 with a step of 10. It was then resampled by five resampling factors, namely, 0.6, 0.8, 1, 1.2 and 1.4 using the *imresize* command of MATLAB. Each of them was again JPEG compressed at quality factor of 90. This was repeated for 5000 images to constitute the training set and a disjoint set of 1000 images for the testing set. Hence the total training set for image dimension  $1024 \times 1024$  was 25000 with each resampling factor having 5000 images. Similarly, the testing set had 5000 images with each resampling factor having 1000 images.

For very large image sizes such as  $4928 \times 3264$ , sometimes the central region could not be cropped and that particular instance was discarded. In this way, with all image sizes, the training set had 75,000 images with all the five resampling factors having images in equal proportion. Similarly, the testing set of 15,000 images was equally divided amongst all five resampling factors. Since this is a case of balanced class distribution, detection accuracy for each resampling factor is taken as the total number of correctly classified images.

**Table 2.** Results on MISLnet [7] for JPEG+Res+JPEG. '-' denotes absence. When trained and tested for a fixed image resolution of  $1024 \times 1024$ , MISLnet’s accuracy surges to 99%. However, when trained and tested simultaneously for varying image resolutions, MISLnet is barely able to go past 90% accuracy.

Patch size / Img Resolution	Resampling Factors					Avg Acc %
	0.6	0.8	1	1.2	1.4	
256 / 512	-	-	-	-	-	-
256 / 1024	99.3	98.8	99.1	99.4	99.0	<b>99.0</b>
256 / Larger	-	-	-	-	-	-
256 / 512	72.3	79.3	98.3	93.0	93.8	87.25
256 / 1024	92.9	80.4	98.3	99.3	98.0	<b>93.60</b>
256 / Larger	89.0	73.5	97.5	96.6	93.4	89.90

**Table 3.** Results for resampling factor detection on double JPEG compressed images. All the listed solutions gave close to 99% accuracy when trained and tested on images of fixed dimension but dropped by 10% when retrained and tested for images of varying dimensions. The proposed solutions, IPN and BN help to regain the lost accuracy. Accuracy in %.

Method	Resampling Factors					
	0.6	0.8	1	1.2	1.4	Avg
MISLnet [7]	84.7	77.7	98.0	96.3	94.9	90.3
Quan <i>et al.</i> [10]	80.4	78.9	97.3	97.1	95.8	89.9
Chen <i>et al.</i> [20]	73.4	79.13	97.3	94	94.9	87.7
MPN	78.3	48.0	93.7	52.3	91.1	72.7
IPN (ours)	98.6	97.1	98.4	94.3	94.8	<b>96.6</b>
BN (ours)	98.4	99.0	98.0	98.8	99.5	<b>98.7</b>

**Table 4.** Patch sizes for the proposed IPN and BN.

Image size $d \times d$	Patch size $p \times p$	
	IPN	BN
$d < 1024$	128	64
$1024 < d < 2000$	256	128
$d > 2000$	512	256

**Table 5.** Patch level accuracy in % for Natural Images (NI) vs. Computer Generated (CG) images of heterogeneous origin on the Columbia dataset [21].

Method	Google NI	Personal NI	CG
Quan <i>et al.</i> [10]	75.8	88.7	68.6
MISLnet [7]	70.2	70.3	49.0
IPN (Ours)	<b>90.0</b>	<b>94.0</b>	<b>78.0</b>

## 4.2. Results on Resampling Detection

The results for resampling detection in double compressed JPEG images are shown in Table 3. When the previous works listed in the table were re-trained on images of fixed base dimension of  $1024 \times 1024$  with patch chosen from image center, the following average accuracies were obtained — MISLnet

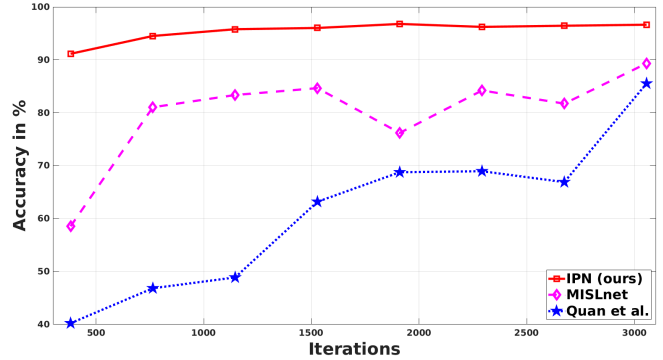


**Fig. 4.** The proposed IPN also converges faster (in about 2000 iterations) for resampling detection task with final accuracy reported in Table 3. The other two methods, MISLnet [7] and Quan *et al.* [10] took up to 6000 iterations to stabilize. The curve for Chen *et al.* [20] not shown because of extremely slow convergence taking 15000+ iterations to converge.

[7]: 98.7%, Quan *et al.* [10]: 98.4% and Chen *et al.* [20]: 98.2%. However, interestingly when they were re-trained on all image sizes about 10% drop in average accuracy can be observed in Table 3. Since these works cannot alter patch size, the default patch size chosen for the architecture was used. It was in the range of 200 – 300. The table next reports the average accuracy obtained by using the adaptive max-pooling operation instead of iterative pooling in IPN. This is referred as the Max-Pooling Network (MPN). As suggested in Sec. 2, it is unable to restore the accuracy. IPN on the other side has very promising results, restoring much of the lost accuracy. Also BN with the help of prior information about the original image size again gives close to 99% average accuracy and with much smaller patch sizes. The choice of patch size for IPN and BN is listed in Table 4.

## 4.3. Results on Photorealism Detection

The flexibility in the choice of patch size is the main strength of the proposed solutions. In this section, we describe some of the added benefits that are obtained by building on top of pre-trained models. Firstly, the convergence for the resampling detection task is much faster, as seen in Fig. 4. Secondly, the CNN model proposed in [4, 7] are better suited for resampling detection task and a few other tasks, while the one proposed in [10] is better suited for photorealism detection. However, by building on top of already existing state-of-the-art architectures helps easy generalization to different problems. For example, by using ResNet-18 [17] as base architecture, IPN achieves better performance for both resampling and photorealism detection tasks as corroborated by Table 3 and Table 5. For Table 5, the exact procedure followed by [10] on the Columbia dataset [21] was used to re-train the listed CNN models, except for one change. The Natural Images (NI) and

**Table 6.** Performance of IPN on JPEG+Res+Rot+JPEG. Rot Clock: Clockwise rotation; Rot Anti: Anti-clockwise rotation; Res Acc: Resampling detection accuracy; Rot Acc: Rotation detection Accuracy; Res 0.6: Resampling by factor of 0.6.

		IPN (ours)	MISLnet [7]	Quan et al. [10]	
Rot Anti	Res 0.6	Res Acc	96.6	83.3	77.9
		Rot Acc	95.2	85.2	38.9
	Res 0.8	Res Acc	93.9	75.5	51.3
		Rot Acc	95.3	82.7	56.8
	Res 1	Res Acc	95	84.8	62.2
		Rot Acc	99.1	86.9	66.5
	Res 1.2	Res Acc	96.6	89.2	52.6
		Rot Acc	98.1	87.5	76.5
	Res 1.4	Res Acc	98.9	96.5	85.4
		Rot Acc	99.3	91.7	75.0
Rot Clock	Res 0.6	Res Acc	96.4	82.1	78.1
		Rot Acc	94.4	85.5	68.0
	Res 0.8	Res Acc	95	75.4	50.5
		Rot Acc	94.8	86.9	51.0
	Res 1	Res Acc	94.9	83.8	61.8
		Rot Acc	98.7	91.6	38.6
	Res 1.2	Res Acc	96.4	90.3	52.7
		Rot Acc	98.3	93.5	26.9
	Res 1.4	Res Acc	99.1	97.5	87.0
		Rot Acc	99.4	94.6	27.4
<b>Resampling Avg Acc %</b>		<b>96.2</b>	85.8	66.0	
<b>Rotation Avg Acc %</b>		<b>97.2</b>	88.6	52.5	

Computer Generated Images (CG) were not resized to a fixed dimension before patch selection. This is to prevent the CNNs from classifying based on the resampling factor. Similarly we test the proposed method for JPEG+Res+Rot+JPEG forgery. For this set up  $1024 \times 1024$  images were rotated clockwise and anti-clockwise in the range  $-20$  degrees to  $+20$  degrees. But for detection only clockwise or anti-clockwise rotation has to be detected. This restriction is made because this is a much harder problem than the one mentioned in Table 3. Rest of the settings remain the same.

## 5. CONCLUSION

Many image forensic problems require to alter the patch size depending on the image size. However, the fully connected layers of CNNs do not allow this. To tackle this issue, we proposed two solutions: IPN and BN. IPN converts variable size tensors to a fixed dimension by iteratively convolving them and BN had dedicated pathways for different image sizes. This helped to restore 7-9% accuracy for resampling detection which was lost by exposing existing solutions to multiple image sizes. We also demonstrated that by building on top of existing state-of-the-art deep learning models such as ResNet18, we obtained stable iterations and faster convergence. This approach also generalizes well for other tasks such as photorealism detection.

## 6. REFERENCES

- [1] A. C. Popescu and H. Farid, "Exposing Digital Forgeries by Detecting Traces of Resampling," *IEEE Transactions on Signal Processing*, vol. 53, no. 2, pp. 758–767, Feb 2005.
- [2] T. Bianchi and A. Piva, "Reverse Engineering of Double JPEG Compression in the Presence of Image Resizing," in *IEEE International Workshop on Information Forensics and Security (WIFS)*, Dec 2012, pp. 127–132.
- [3] S. Sahu and M. Okade, "Exposing Image Resizing utilizing Welch Power Spectral Density Analysis for Double Compressed JPEG Images," in *International Workshop on Information Forensics and Security (WIFS)*, Dec 2018, pp. 1–6.
- [4] B. Bayar and M. C. Stamm, "On the Robustness of Constrained Convolutional Neural Networks to JPEG Post-Compression for Image Resampling Detection," in *IEEE International Conference on Acoustics, Speech and Signal Processing (ICASSP)*, March 2017, pp. 2152–2156.
- [5] A. C. Gallagher, "Detection of Linear and Cubic Interpolation in JPEG Compressed Images," in *The 2nd Canadian Conference on Computer and Robot Vision (CRV'05)*, May 2005, pp. 65–72.
- [6] Alessandro Piva, "An Overview on Image Forensics," *ISRN Signal Processing*, vol. 2013, pp. 1 – 22, Oct 2012.
- [7] B. Bayar and M. C. Stamm, "Constrained Convolutional Neural Networks: A New Approach Towards General Purpose Image Manipulation Detection," *IEEE Transactions on Information Forensics and Security*, vol. 13, no. 11, pp. 2691–2706, Nov 2018.
- [8] H. Jain, J. Das, H. K. Verma, and N. Khanna, "An Enhanced Statistical Approach for Median Filtering Detection Using Difference Image," in *IEEE International Conference on Identity, Security and Behavior Analysis (ISBA)*, Feb 2017, pp. 1–7.
- [9] Vinay Verma, Nikita Agarwal, and Nitin Khanna, "DCT-Domain Deep Convolutional Neural Networks for Multiple JPEG Compression Classification," *Signal Processing: Image Communication*, vol. 67, pp. 22 – 33, Sep 2018.
- [10] W. Quan, K. Wang, D. Yan, and X. Zhang, "Distinguishing Between Natural and Computer-Generated Images Using Convolutional Neural Networks," *IEEE Transactions on Information Forensics and Security*, vol. 13, no. 11, pp. 2772–2787, Nov 2018.

- [11] S. Ren, K. He, R. Girshick, and J. Sun, "Faster R-CNN: Towards Real-Time Object Detection with Region Proposal Networks," *IEEE Transactions on Pattern Analysis and Machine Intelligence*, vol. 39, no. 6, pp. 1137–1149, June 2017.
- [12] Maximilian Riesenhuber and Tomaso Poggio, "Hierarchical Models of Object Recognition in Cortex," *Nature neuroscience*, vol. 2, no. 11, pp. 1019, 1999.
- [13] Alex Krizhevsky, Ilya Sutskever, and Geoffrey E Hinton, "ImageNet Classification with Deep Convolutional Neural Networks," in *Advances in Neural Information Processing Systems (NIPS)*, 2012, pp. 1097–1105.
- [14] H. Li, W. Luo, X. Qiu, and J. Huang, "Identification of Various Image Operations Using Residual-Based Features," *IEEE Transactions on Circuits and Systems for Video Technology*, vol. 28, no. 1, pp. 31–45, Jan 2018.
- [15] M. Kirchner and T. Gloe, "On Resampling Detection in Re-Compressed Images," in *IEEE International Workshop on Information Forensics and Security (WIFS)*, Dec 2009, pp. 21–25.
- [16] Joseph Redmon, Santosh Divvala, Ross Girshick, and Ali Farhadi, "You Only Look Once: Unified, Real-Time Object Detection," in *The IEEE Conference on Computer Vision and Pattern Recognition (CVPR)*, June 2016.
- [17] Kaiming He, Xiangyu Zhang, Shaoqing Ren, and Jian Sun, "Deep Residual Learning for Image Recognition," in *The IEEE Conference on Computer Vision and Pattern Recognition (CVPR)*, June 2016.
- [18] Duc-Tien Dang-Nguyen, Cecilia Pasquini, Valentina Conotter, and Giulia Boato, "RAISE: A Raw Images Dataset for Digital Image Forensics," in *Proceedings of the 6th ACM Multimedia Systems Conference*. 2015, pp. 219–224, ACM.
- [19] "An Open Source Machine Learning Framework," <https://pytorch.org>, Accessed: 2019.
- [20] Yifang Chen, Xiangui Kang, Yun Q. Shi, and Z. Jane Wang, "A Multi-Purpose Image Forensic Method using Densely Connected Convolutional Neural Networks," *Journal of Real-Time Image Processing*, vol. 16, no. 3, pp. 725–740, June 2019.
- [21] T.-T Ng, S.-F. Chang, J. Hsu, and M. Pepeljugoski, "Columbia Photographic Images and Photorealistic Computer Graphics Dataset," Tech. Rep., ADVENT, Columbia University, 2004.